International Journal of Bridge Engineering (IJBE), Special Issue 2017, pp. 99-123

SEISMIC DESIGN OF PRECAST PIERS WITH POCKET CONNECTIONS, CFRP TENDONS AND ECC/UHPC COLUMNS

Alireza Mohebbi [1], M. Saiid Saiidi [2] and Ahmad M. Itani[3]

[1,2,3] University of Nevada, Reno, Dept. of Civil and Environmental Engineering, USA
e-mail: mohebbi@nevada.unr.edu, saiidi@unr.edu, itani@unr.edu

ABSTRACT: States in moderate and high seismic zones have not been able to embrace accelerated bridge construction (ABC) because of insufficient research results and guidelines for seismic design of prefabricated members and connections. The primary objectives of this paper were to present preliminary seismic design methods for (1) square column-cap beam pocket connections, (2) square column-footing pocket connections, (3) unbonded carbon fiber reinforced polymer (CFRP) tendons for post-tensioned bridge columns, and (4) plastic hinge zones with ultra-high performance concrete (UHPC), and engineered cementitious composite (ECC). The design methods were developed based on results of previous studies on ABC connections and those conducted as part of a current experimental and analytical investigation. The seismic provisions of the American Association of State Highway and Transportation Officials (AASHTO) were utilized where appropriate. A summary of the shake table tests and analytical investigations of precast bents with pocket (socket) connections and advanced materials that were used in developing the design methods is also presented. Three design examples illustrating different steps of the proposed methods are discussed.

KEYWORDS: Accelerated bridge construction (ABC), Carbon fiber reinforced polymer (CFRP) tendon, Engineered cementitious composite (ECC), Pocket (socket) connections, Ultra-high performance concrete (UHPC).

1 INTRODUCTION

Much research has been conducted investigating the advantages of accelerated bridge construction (ABC) for bridge owners, contractors, construction workers, and the travelling public [1-5]. ABC expedites bridge construction by using prefabricated reinforced concrete members normally constructed offsite under controlled environmental conditions and assembled onsite, although some components might be site-cast. Different methods have been developed to connect prefabricated reinforced concrete members in which pocket (also known as socket) connections constitute some of the promising methods [6-7].

Pocket connections are used for precast-to-precast or precast-to-cast in place elements with reinforced concrete members inserted into adjacent members and connected with grout or concrete [7-9]. It is critical in this type of connection that sufficient embedment length is provided to develop the full capacity of the connected members and maintain the structural integrity under extreme loads.

ABC also provides the opportunity for advanced and damage-resistant materials to be incorporated in the prefabricated bridge components. Advanced materials with superior engineering properties can improve the seismic performance of bridges under strong earthquakes and reduce damage [10-11]. Ultra-high performance concrete (UHPC) and engineered cementitious composite (ECC) are advanced cementitious material having approximately 2% volumetric ratio of steel and polyvinyl alcohol (PVA) fibers, respectively. Fibers in UHPC and ECC provide tensile strain capacity and confinement and prevent materials from spalling that can reduce plastic hinge damage under extreme earthquakes. Carbon fiber reinforced polymer (CFRP) is another attractive advanced material because it is noncorrosive with relatively high tensile strength capacity. Unbonded CFRP tendons can be used as an alternative to unbonded post-tensioning steel tendons in bridge columns to reduce permanent displacement under seismic loads.

Despite the numerous advantages, states in moderate and high seismic zones have not been able to embrace ABC extensively because of insufficient research results and guidelines for seismic design of prefabricated members and connections. The overall objective of this study was to help address this gap. The study involved shake table testing of two large-scale precast bents with pocket connections and advanced materials and finite element modeling. Details of that part of the study were presented elsewhere. The main objectives of part of the study presented in this article were to develop a step-by-step seismic design guideline for: (1) square column-cap beam pocket connections, (2) square column-footing pocket connections, (3) unbonded CFRP tendons for post-tensioned bridge columns, and (4) plastic hinge zones with UHPC/ECC. A summary of the other parts of the study is included for completeness. The design methods presented in this article are further illustrated in three design examples.

2 SUMMARY OF EXPERIMENTAL STUDIES

Two 1/3 scale models of bridge piers consisting of precast components with pocket connections and advanced materials were constructed and tested on a shake table at the Earthquake Engineering Laboratory at the University of Nevada, Reno. The first model was a single column and the second was a two-column pier. A summary of the innovations incorporated in the design of the models and key experimental results are presented.

2.1 Single column model

A square precast column was constructed and post-tensioned with unbonded CFRP tendons. The column was connected to a precast footing incorporating a pocket. UHPC was used in the plastic hinge zone of the column to mitigate seismic damage over a height equal to twice the column cross-sectional dimension starting from the column-footing interface. UHPC was also used in the pocket connection to fill the gap between the column and the footing. The embedment length of the column in the footing pocket was the same as the column cross sectional dimension. Details of the column-footing pocket connection are shown in *Fig.1*. Eight diagonal bars were included in the footing top reinforcement at 45 degree angle around the pocket as shown in *Fig.2*. These bars were utilized to eliminate potential cracks due to stress concentration at the corners of the pocket. More detailed information on the column model, post-tensioning with CFRP tendons, test setup, instrumentations, and loading protocol is presented in Mohebbi et al. [12-13].

The column was subjected to successive motions simulating scaled versions of the 1994 Northridge-Rinaldi earthquake until failure. The column model reached a maximum drift ratio of 6.9%, displacement ductility of 13.8, and negligible residual drift even under the motion with amplitude that was twice the design earthquake amplitude. Results showed that the pocket connection performed well and the embedment length of the column in the footing was sufficient to develop plastic moment at the base of the column. CFRP tendons effectively eliminated residual drifts under strong earthquakes. UHPC reduced the plastic hinge damage with the apparent damage under the design earthquake being minor spalling of cover UHPC and a crack at the column-footing interface. The maximum measured tensile strain in the diagonal bars was 25% of the yield strain, which is sufficiently high to indicate that the diagonal bars were engaged and played a role in preventing cracking while undergoing strains that were well below the yield strain. This result was consistent with the apparent damage where no cracks were observed in the footing pocket and at the corners.

2.2 Two-column bent model

The bent consisted of two precast square columns one with UHPC and the other with ECC in the plastic hinge zones. Conventional concrete was used elsewhere. The height of UHPC/ECC in the plastic hinge zones was 1.5 times the column cross-sectional dimension. The columns were connected to a precast footing and a precast cap beam using circular and square pocket connections, respectively. High-strength, non-shrink grout was used in the pockets to fill the gap around the columns in the pockets. The columns had moment connections at the top and two-way hinge connections at the bottom. Details of the cap beam and footing reinforcement are shown in *Fig.3* and

Fig.4, respectively. Unlike conventional reinforced concrete cap beams with bottom reinforcement distributed across the beam section, the bottom longitudinal bars were bundled and placed outside the pockets to avoid interference with the columns. Two headed diagonal bars were placed at the level of the cap beam bottom reinforcement at 45 degrees around the pockets to eliminate potential cracks due to stress concentration at the corners. In addition, stirrups and spirals were placed around the cap beam and the footing pockets over the lower and upper half of the height of the pockets, respectively, to provide confinement at the joints. The embedment length of the column in the cap beam pockets was 1.0 times the column cross sectional dimension. More details about the bent model, test setup, instrumentations, and loading protocol are presented in Mohebbi et al. [14].

The bent was subjected to successive earthquake motions simulating scaled versions of the 1994 Northridge-Sylmar earthquake in the shake table tests. The bent model reached a drift ratio of 9.6% and a displacement ductility of 12 under 150% design earthquake, during which the top plastic hinges failed. The structural integrity was maintained during the entire test. The results demonstrated that the embedment length of the column in the cap beam pockets was sufficient to develop the column plastic moment below the cap beam. ECC and UHPC effectively reduced the plastic hinge damage under the design earthquake.

However, a different damage state was observed in the two columns under the 150% design earthquake. The damage in the ECC column was in the plastic hinge whereas the damage in the UHPC column was in the connection to the cap beam. The high stiffness and strength of UHPC relative to ECC increased the flexural demand and damage in the cap beam adjacent to UHPC under the 150% design earthquake. The maximum measured tensile strain in the diagonal bars around the cap beam pocket was 37% of the yield strain, indicating that the diagonal bars were mobilized and were effective in eliminating cracks at the corners. The maximum tensile strain in the stirrups around the cap beam pockets was negligible during the test. The low strains indicate that sufficient confinement was provided by the column transverse reinforcement and the bottom diagonal bars in the cap beam. It was concluded that there was no need to provide more confinement at the joints by placing stirrups in the cap beam around the pockets. Elimination of these ties reduces rebar congestion and simplifies construction of the cap beam. The tensile strain in the spirals around the footing pocket was also negligible because the column-footing connection was a two-way hinge connection, and a relatively small moment was transferred to the footing. Therefore, it was concluded that spirals around the hinge pocket connections were not necessary.

3 ANALYTICAL STUDIES

The main purpose of the analytical studies reported in this article was to investigate the effect of the column section geometry on stress distribution of the column-cap beam connection. Another objective was to determine if additional cap beam reinforcement beyond that used in the test model is necessary in square column connections.

3.1 Analytical modelling

A three-dimensional (3D) elastic finite element model of a column-cap beam connection was developed using SAP 2000 [15]. The model consisted of a portion of the two-column bent model described earlier in section 2.2 from the point of the contraflexure in the column to the mid span of the cap beam. The modeling details and element discretization are shown in *Fig. 5*. A pin support was assigned to the point of contraflexure at the column and a roller support was assigned to the center of the cap beam to constrain vertical displacement. Solid elements with conventional concrete were used to model the column-cap beam connection. The compressive strength of concrete was assumed to be 34.5 MPa (5 ksi). Two geometries of the column, a square section and an equivalent circular section, were analyzed to investigate the effect of the column section geometry on stress distribution of the column-cap beam connection. The cross-sectional dimension of the squarer column was 355.6 x 355.6 mm (14 x 14 in) and the diameter of the equivalent circular column was 401.3 mm (15.8 in). Vertical loads, P_D, of 98.8 kN (22.2 kips) were applied to the model at the location of each steel girders that were used in the test setup of the two-column bent model. Another vertical load, P_O, of 342.5 kN (77 kips) was applied to the cap beam passing through the center of the column to account for the overturning effect in the bent model under the ultimate drift. A lateral load, V, of 324.7 kN (73 kips) was applied to the center of the cap beam on the left side. This load matched the measured lateral load capacity of the two-column bent model. The applied loads were distributed uniformly over the width of the cap beam at each location.

3.2 Analytical results

Contour of the maximum tensile stress in the column-cap beam connections for the square and circular columns under the combined horizontal and vertical loads are shown in *Fig. 6*. The right side of the columns was under tension and the left side was under compression due to the applied loads. The tensile stress distribution in the cap beam was approximately uniform in the case with square column but sinusoidal in the other case. *Figure 7* shows the maximum tensile stresses at the column-cap beam interfaces. Comparison of the results shows that high tensile stresses were concentrated at the corners of the square column while the maximum tensile stress was at the center of the circular column. The

tensile stress distribution at section A-A located at the interface of the column cap beam is shown in *Fig. 8*. According to the results, the maximum tensile stress at the center of the square column was 11% less than that of the circular column while the maximum tensile stress at the corners of the square column was 63% higher than that of the circular column. Results reveal that there is a considerable stress concentration in the cap beam at the corners of the square column. Although, the model was developed for monolithic column-cap beam connections, the results can be inferred for precast columns. Analytical results were consistent with the measured data in the single column and the two-column bent models where diagonal bars were mobilized around the square pockets. Therefore, to design square pocket connections, diagonal reinforcement is recommended around square pockets to eliminate damage due to the stress concentrations at the corners.

4 PROPOSED SEISMIC DESIGN METHODS

Seismic design methods for square and rectangular column-cap beam pocket connections, square and rectangular column-footing pocket connections, and unbonded CFRP tendons for post-tensioned bridge columns were developed based on the experimental results and the analytical investigations. Rectangular columns are included because it was believed that the research results are applicable to both square and rectangular columns. Recommendations were also developed for UHPC/ECC length in column plastic hinge zones. The design steps in each method were illustrated in three examples that are summarized in the appendix.

4.1 Design of square and rectangular column-cap beam pocket connections

A step-by-step design procedure for square column-cap beam pocket connections was developed as follows:

- Step 1. Determine the pocket dimension (B_P)

The plan view dimension of the square pocket should be determined according to Eq. (1).

$$B_P = B_C + 2\mathrm{Gap} \tag{1}$$

where: B_C is the column dimension,
Gap is the space between the column and the pocket face. The gap should not be less than 38 mm (1.5 in) and should not exceed 102 mm (4 in)

- Step 2. Determine the minimum pocket depth (D_P)

The depth of the pocket should be at least the greatest of those in Equations 2-4. Equation (2) was developed based on the experimental results. Equation (3) was developed according to the minimum development length of straight

reinforcing steel in AASHTO [16]. Equation (4) was developed by Motaref et al. [17].

$$D_p \geq \begin{cases} 1.0\,B_c + \text{Gap} & (2) \\ \dfrac{0.79 d_b f_{ye}}{\sqrt{f'_c}} + \text{Gap} & (3) \\ \dfrac{1.56 V_{PO} + \sqrt{4.74 {V_{PO}}^2 + 6.22 M_{PO} f'_c B_c}}{B_c f'_c} + \text{Gap} & (4) \end{cases}$$

where: d_b is the diameter of the column longitudinal bar (in),
f_{ye} is the expected yield stress of longitudinal reinforcement (ksi),
f'_c is the nominal compressive strength of concrete (ksi),
V_{PO} is the shear force corresponding to column plastic overstrength moment (kip),
M_{PO} is the column plastic overstrength moment (kip.in),

- Step 3. Determine the minimum cap beam depth (D_{Cap})

The depth of the cap beam above the pocket should be sufficiently large to avoid punching shear failure above the pocket due to the weight of the cap beam. The cap beam depth of $1.25D_P$ may be used for the initial design and should be checked when the design is finalized [9].

- Step 4. Determine the minimum cap beam width (W_{Cap})

The cap beam should extend 305 mm (12 in) on each side of the column according to AASHTO [16]. The minimum width of the cap beam is as follows:

$$W_{Cap} = B_C + 610 \text{ mm } (24 \text{ in}) + 2\text{Gap} \quad (5)$$

- Step 5. Opening for pumping grout (W_V)

An opening should be left at the top of the cap beam pocket for placing grout or UHPC. The side dimension/diameter of the opening should be at least 102 mm (4 in). The inner face of the pocket at the top should be sloped 5 to 10% to eliminate air entrapment during placement of grout or UHPC.

$$W_V \geq 102\ mm\ (4\ in) \quad (6)$$

- Step 6. Design of cap beam longitudinal reinforcement

The cap beam longitudinal reinforcement should be designed according to AASHTO [16]. The bottom longitudinal bars should be bundled and placed outside the pocket to avoid interference with the precast columns. Section analysis of the cap beam should be performed based on the nominal properties of the concrete and reinforcement. The size of the longitudinal bars should be adjusted such that the moment demand in the cap beam is less than the effective yield moment of the beam section. Additional longitudinal reinforcement at the bottom should be placed outside the pocket to satisfy shrinkage and temperature reinforcement according to section 5.10.8 of AASHTO [18]. The ends of the

additional longitudinal bars should be bent and satisfy specification on the standard hooks according to section 5.10.2 of AASHTO [18].

$$M_{y(eff)} > M_{Demand} \quad (7)$$

where: $M_{y(eff)}$ is the effective yield moment of the cap beam section,
M_{Demand} is the maximum moment demand in the cap beam

- Step 7. Design of cap beam transverse reinforcement

Vertical stirrups inside and outside the pocket connection should satisfy AASHTO requirements in section 8.13.5.1 [16]. Vertical stirrups with a total area (A_{VO}) outside the pocket connection should satisfy Eq. (8) and should be placed within a distance equal to the column diameter (or the maximum side dimension for square or rectangular columns) extending from each side of the column in addition to the transvers steel for shear in the cap beam. Vertical stirrups with a total area (A_{Vi}) inside the pocket connection should satisfy Eq. (9). No horizontal J-bars are required in the design of the cap beam pocket connections.

$$A_{VO} \geq 0.175A_{st} \quad (8)$$

$$A_{Vi} \geq 0.135A_{st} \quad (9)$$

where: A_{st} is the total area of column reinforcement anchored in the joint.

- Step 8. Design of diagonal reinforcement

According to the experimental results and analytical investigations discussed in this article, diagonal bars around the square pockets are required to help resist tensile stresses at the corners. The area of the diagonal bars should be one-third of the required bottom longitudinal bar area of the cap beam at the column face. The diagonal bars should be placed at 45 degree relative to the longitudinal axis of the cap beam. The length of the diagonal bars from the corner of the pocket to the end of the bars should satisfy the minimum development length of reinforcing steel according to AASHTO [16].

$$A_{s(Diagonal)} \geq (\frac{1}{3}A_{sb(Cap)})/2 = \frac{1}{6}A_{sb(Cap)} \quad (10)$$

where: $A_{s(Dialonal)}$ is the area of the diagonal bars at each side of the pocket,
$A_{sb(Cap)}$ is the total area of the required bottom longitudinal bars of the cap beam at the column face,

- Step 9. Principal stress checks

Moment-resisting joints should satisfy the AASHTO requirements in section 8.13.2 [16].

4.2 Design of square and rectangular column - footing pocket connections

A step-by-step design procedure of square column-footing pocket connections

was developed as follows:

- Step 1. Determine the minimum pocket dimension (B_P)

The plan view dimension of the footing pocket should be determined according to Eq. (1) described in section 4.1.

- Step 2. Determine the minimum pocket depth (D_P)

The minimum pocket depth should be determined based on the Eq. (2) to Eq. (4).

- Step 3. Determine the minimum footing depth ($D_{Footing}$)

The depth of the footing should be sufficiently large to avoid punching shear failure below the pocket due to the weight of the column. The footing depth of 1.25 D_P may be used in the initial design.

- Step 4. Design of footing longitudinal reinforcement

Spread footings should be designed according to section 6.3 of AASHTO [16]. The bottom longitudinal bars should be distributed across the bottom of the footing. The top longitudinal bars should be placed outside the pocket to avoid interference with the precast columns. Section analysis of the footing should be performed based on the nominal properties of the concrete and reinforcement. The size of the longitudinal bars should be adjusted such that the flexural demand at the face of the column is less than the effective yield moment of the footing section. Additional longitudinal reinforcement should be placed outside the pocket to satisfy shrinkage and temperature reinforcement. The ends of the additional longitudinal bars should be bent and satisfy specification on the standard hooks.

- Step 5. Design of diagonal reinforcement

The area of the diagonal bars should be at least one-third of the required top longitudinal bar area of the footing. The diagonal bars should be placed at 45 degree relative to the longitudinal axis of the footing. The spacing of the diagonal bars should not exceed 4.0 times the bar diameter. The length of the diagonal bars from the corner of the pocket to the ends of the bars should satisfy the minimum development length of reinforcing steel according to section 8.8.4 of AASHTO [16].

- Step 6. Resistance to overturning

The overturning demand in spread footings should satisfy section 6.3.4 of AASHTO [16].

- Step 7. Resistance to sliding

The lateral demand due to the plastic overstrength shear of the column should satisfy section 6.3.5 of AASHTO [16].

- Step 8. Shear design

Shear demand in the spread footings should satisfy sections 6.3.7 and 6.4.7 of AASHTO for the shear design [16].

- Step 9. Principal stress checks

Footing to column moment resisting joints should satisfy the requirements of

section 6.4.5 of AASHTO [16].

4.3 Design of unbonded CFRP tendons for post-tensioned bridge columns

A step-by-step design procedure for post-tensioned bridge columns using unbonded CFRP tendons was developed as follows:

- Step 1. Determine the initial post-tensioning stress (f_{pi})

Initial posttensioning stress after short and long term losses should be 25% of the guaranteed capacity of the CFRP tendons specified by the manufacturer.

$$f_{pi} = 0.25 f_u \tag{11}$$

where: f_u is the maximum guaranteed tensile stress of CFRP tendons

- Step 2. Determine the area of CFRP Tendons (A_{CFRP})

The total area of the CFRP tendons for the initial design should be determined such that the initial posttensioning force is approximately equal to the column axial force due to the dead load. Experimental results have shown that this level of prestress is sufficient to control residual displacements.

$$ALI = P/(f'_c A_g) \tag{12}$$

$$A_{CFRP} = ALI f'_c A_g / (0.25 f_u) = P/(0.25 f_u) \tag{13}$$

where: ALI is the axial load index,
P is the maximum compressive force acting on the column due to dead load,
f'_c is the nominal compressive strength of concrete,
A_g is the gross cross-sectional area of the column

- Step 3. Pushover analysis

Pushover analysis of the post-tensioned column should be performed and the tensile stress in the CFRP tendons should be recorded. Experimental results have revealed that the tensile stress in the tendons increased as the lateral displacement of the column increases due to the elongation of the tendons [13]. Therefore, the area of the CFRP tendons should be adjusted such that the maximum tensile stress in the tendons is less than 80% of the guaranteed capacity of the tendons at the column failure.

$$f_{Max(CFRP)} \leq 0.8 f_u \tag{14}$$

where: $f_{Max(CFRP)}$ is the maximum tensile stress in CFRP tendons at the column failure

4.4 Design of plastic hinge zones with UHPC/ECC

The experimental results showed that UHPC and ECC reduced the plastic hinge damage under strong earthquakes [14]. The height of UHPC/ECC in the column plastic hinge zones is recommended to be determined such that the

moment in the column section with conventional concrete is 75% of the plastic moment of the column section with UHPC/ECC. The height of UHPC/ECC should not be less than 1.0 times the column maximum cross-sectional dimension or diameter. Confined properties of ECC should be determined according to the method proposed by Motaref et al. [17]. Because no models are available to calculate confined properties of UHPC with transverse steel at the time of this writing, Mander's model [19] is recommended to be used. In addition, due to the high bond strength of UHPC/ECC, the column longitudinal bars in the plastic hinge zones should be debonded to distribute the plastic deformation along the bars and prevent premature rebar rupture due to stress concentration. Debonding the longitudinal bars in the plastic hinge zones increases the drift capacity of the columns. The debonded length of the longitudinal bars is tentatively recommended to be determined such that the moment demand at the end of the debonded length in the column is 80% of the column plastic moment. This recommendation was confirmed in the tests [13-14].

5 CONCLUSIONS

Seismic design methods for use in accelerated bridge construction (ABC) were developed utilizing the results from this and previous studies integrated with many of the AASHTO provisions for cast-in-place bridges. The proposed methods included the design of the square/rectangular column-cap beam pocket connections, square/rectangular column-footing pocket connections, and unbonded CFRP tendons for post-tensioned bridge columns. Recommendations were also developed for UHPC/ECC length in column plastic hinge zones. The proposed design methods are practical as demonstrated in the three design examples presented in the appendix of this paper.

ACKNOWLEDGMENTS

The project was supported by the US Department of Transportation contract no. DTRT13-GUTC41 through the Accelerated Bridge Construction University Transportation Center (ABC-UTC) with Florida International University (lead), the Iowa State University, and the University of Nevada, Reno. The authors would like to thank Lafarge North America Inc. for donating UHPC material, Tokyo Rope Inc. for providing CFRP tendons, Nevada Department of Transportation for partial support of the project, and UNR lab staff for conducting the experiments.

REFERENCES

[1] Marsh, M.L., Wernli, M., Garrett, B.E., Stanton, J.F., Eberhard, M.O., and Weinert, M.D, "Application of Accelerated Bridge Construction Connections in Moderate-to-High Seismic Regions." National Cooperative Highway Research Program, Washington, D.C., NCHRP

Report No. 698, 2011.
[2] Haber, Z, Saiidi, M, and Sanders, D, "Precast Column-Footing Connections for Accelerated Bridge Construction in Seismic Zones", Center for Civil Engineering Earthquake Research, Department of Civil and Environmental Engineering, University of Nevada, Reno, Nevada, Report No. CCEER-13-08, May, 2013.
[3] Tazarv, M., and Saiidi, M, "Low-Damage Precast Columns for Accelerated Bridge Construction in High Seismic Zones", J. Bridge Eng., 10.1061/(ASCE)BE.1943-5592.0000806, 04015056, 2015.
[4] Mehraein, M., and Saiidi, M, "Seismic Performance of Bridge Column-Pile-Shaft Pin Connections for Application in Accelerated Bridge Construction." Rep. No. CCEER-16-01, Center for Civil Engineering Earthquake Research, Dept. of Civil and Environmental Engineering, University of Nevada, Reno, NV, 2016.
[5] Thonstad, T., Mantawy, I.M., Stanton, J.F., Eberhard, M.O., Sanders, D.H, "Shaking Table Performance of a New Bridge System with Pre-Tensioned, Rocking Columns", Journal of Bridge Engineering, ASCE, 21(4), 04015079, 2016.
[6] Mehrsoroush, A., and Saiidi, M, "Cyclic Response of Precast Bridge Piers with Novel Column-Base Pipe Pins and Pocket Cap Beam Connections", Journal of Bridge Engineering, 10.1061/(ASCE)BE.1943-5592.0000833, 04015080, 2016.
[7] Haraldsson, O. S., Janes, T. M., Eberhard, M. O., and Stanton, J. F, "Seismic resistance of socket connection between footing and precast column", Journal of Bridge Engineering, 18(9), 910-919, 2013.
[8] Larosche, A., Cukrov, M., Sanders, D., and Ziehl, P, "Prestressed Pile to Bent Cap Connections: Seismic Performance of a Full-Scale Three-Pile Specimen", Journal of Bridge Engineering, ASCE, Vol. 19, No. 3, 10 pp, 2014.
[9] Tazarv, M. and Saiidi, M., "Design and Construction of Precast Bent Caps with Pocket Connections for High Seismic Regions," Center For Civil Engineering Earthquake Research, Department Of Civil and Environmental Engineering, University of Nevada, Reno, Nevada, Report No. CCEER-15-06, August 2015.
[10] Saiidi, M., Mohebbi, A., Itani, A., Tazarv, M., and Varela, S, "New Horizons in Seismic Design of Highway Bridges with Advanced Materials and Construction Methods", 14th International Symposium on Structural Engineering, Keynote Paper, No. 10, Beijing, China, 2016.
[11] Varela, S., and Saiidi, M, "Dynamic Performance of Novel Bridge Columns with Superelastic CuAlMn Shape Memory Alloy and ECC", International Journal of Bridge Engineering, Vol. 2 No. 3, pp. 29-58, 2014.
[12] Mohebbi, A., Saiidi, M., and Itani, A, "Self-centering bridge column with CFRP tendons under seismic loads." Proceedings of 8th International Conference on Bridge Maintenance, Safety and Management, Foz do lguacu, Brazil, 2016.
[13] Mohebbi, A., Saiidi, M., and Itani, A, "Shake Table Studies and Analysis of a PT/UHPC Bridge Column with Pocket Connection", ASCE Journal of Structural Engineering, (under review), 2017.
[14] Mohebbi, A., Saiidi, M., and Itani, A, "Shake Table Studies and Analysis of a Precast Two-Column Bent with Advanced Materials and Pocket Connections", ASCE Journal of Bridge Engineering, (under review), 2017.
[15] SAP2000, CSI Computer & Structures Inc. Linear and nonlinear static and dynamic analysis of three-dimensional structures. Berkeley (CA): Computer & Structures, Inc., V18.1.1, 2015.
[16] American Association of State Highway and Transportation Officials (AASHTO), "AASHTO Guide Specifications for LRFD Seismic Bridge Design", Washington, D.C., 2015.
[17] Motaref, S. Saiidi, M., and Sanders, D, "Seismic Response of Precast Bridge Columns with Energy Dissipating Joints", Rep. No. CCEER-11-01, Center for Civil Engineering Earthquake Research, Dept. of Civil and Environmental Engineering, University of Nevada,

Reno, NV, 2011.
[18] American Association of State Highway and Transportation Officials (AASHTO). "AASHTO LRFD Bridge Design Specifications", 5th Edition, 2010.
[19] Mander, J. B., Priestley, M. J. N., and Park, R, "Theoretical stress strain model for confined concrete", Journal of Structural Engineering, 10.1061/(ASCE) 0733-9445(1988)114:8(1804), 1804–1826, 1988.
[20] Mohebbi, A., Saiidi, M., and Itani, A, "Development and Seismic Evaluation of Pier Systems w/Pocket Connections, CFRP Tendons, and ECC/UHPC Columns", Rep. No. CCEER-17-02 Center for Civil Engineering Earthquake Research, Department of Civil and Environmental Engineering, University of Nevada, Reno, NV, 2017.

APPENDIX

Numerical design examples to illustrate different steps of the proposed seismic design methods discussed in section 4 are presented in this appendix. More details about the design examples are presented in Mohebbi, et al. [20].

A.1 Design example for square column-cap beam pocket connections

A multi-bridge column bent with the column dimensions of 42x42 in (1067x1067 mm) has 24 #9 (24 #29) longitudinal bars. The column plastic overstrength moment (M_{PO}) is 4800 k.ft (6508 kN.m), and the shear force corresponding to the plastic overstrength moment (V_{PO}) is 390 kips (1735 kN). The maximum column axial load including overturning effect is 800 kips (3559 kN). The maximum moment, shear, and axial force in the cap beam are 6600 k.ft (8948 kN.m), 950 kips (4226 kN), and 470 kips (2091 kN), respectively. The nominal and expected compressive strength of concrete are 5 ksi (34.5 MPa) and 6.5 ksi (44.8 MPa), respectively. The nominal and expected yield stresses of the steel reinforcement are 60 ksi (414 MPa), and 68 ksi (469 MPa), respectively. The cover concrete is 2 in (51 mm). The required shear reinforcement in the cap beam is 4.5 in^2/ft (9525 mm^2/m). The final design of the cap beam pocket connection is shown in *Fig. 9*.

- Step 1. Determine the minimum pocket plan view dimension (B_P)

Select $\text{Gap} = 2$ in (51mm), $B_P = 42 + 2(2) = 46$ in (1168.4 mm)

- Step 2. Determine the minimum pocket depth (D_P)

$d_{b\#9} = 1.128$ in (28.65 mm)

$$D_p \geq \begin{cases} 42 + 2 = 44 \text{ in (1117.6 mm)} \\ \dfrac{0.79\,(1.128)(68)}{\sqrt{5}} + 2 = 29.1 \text{ in (739.14 mm)} \\ \dfrac{1.56(390) + \sqrt{4.74\,(390^2) + 6.22(4800 \times 12)(5)(42)}}{(42)(5)} + 2 \\ = 46.4 \text{ in (1178.6 mm)} \end{cases}$$

Select $D_P = 48$ in (1219 mm)

- Step 3. Determine the minimum cap beam depth (D_{Cap})

$D_{Cap} = 1.25(48) = 60$ in (1524 mm)

- Step 4. Determine the minimum width of cap beam (W_{Cap})

$W_{Cap} = 42 + 24 + 2(2) = 70$ in (1778 mm)

Select $W_{Cap} = 72$ in (1828.8 mm)

- Step 5. Opening for pumping grout (W_V)

Select a square opening with $W_V = 4\ in$ (101.6 mm)

- Step 6. Design of cap beam longitudinal reinforcement

According to the section analysis of the cap beam in *Fig. 9*, the effective yield moment of the section A-A was calculated using the nominal material properties.

$M_{y\ (eff)} = 6930$ k. ft (9395.8 kN. m)

$M_{Demand-Cap\ Beam} = 6600$ k. ft (8948 kN. m)

$M_{y\ (eff)} \geq M_{Demand-Cap\ Beam}$ OK, select 12 #10 (12 #32) longitudinal bars at the top and bottom and total 6 #10 (6 #32) for skin bars (section A-A in *Fig. 9*).

Additional bottom longitudinal reinforcement outside the pocket was determined according to section 5.10.8 of AASHTO LRFD Bridge Design Specifications.

$$A_{s\ (additional)} = \frac{1.3W_{Cap}D_{Cap}}{2(W_{Cap} + D_{Cap})f_y} = \frac{1.3(70)(60)}{2(70 + 60)(60)} = 0.35\ \frac{in^2}{ft}$$

$$0.11\frac{in^2}{ft} \leq A_{s\ (additional)} \leq 0.6\ \frac{in^2}{ft}$$

$A_{b6} = 0.44\ in^2$ (284 mm^2)

Select #6 @ 12 in (#19 @ 305 mm)

- Step 7. Design of cap beam transverse reinforcement

Vertical stirrups outside the pocket connection (A_{VO}):

$A_{b\#9} = 1.0\ in^2 (645 mm^2)$

$A_{VO} \geq 0.175A_{st} = 0.175(24)(1.0) = 4.2\ in^2$ (2709.7 mm^2)

$$A_{VO/ft} \geq \frac{A_{VO}}{B_C} = 4.2/3.5 = 1.2\ in^2/ft$$

$A_{VR/ft} = 4.5\ in^2/ft$ (Required shear reinforcement in the cap beam)

$A_{VO(total)} \geq A_{VO/ft} + A_{VR/ft} = 1.2 + 4.5 = 5.7\ in^2/ft$ (12065 mm^2/m)

Select #6 @ 5 in (#19 @ 127 mm) stirrups with six vertical legs within the distance B_C=42 in (1067 mm) on each side of the column

$$A_{VO} = \frac{NA_{b\#6}}{S} = \frac{(6)(0.44)}{5/12} = 6.34\ in^2/ft \geq A_{VO(total)}\ \text{OK}$$

Select #6 @ 7 in (#19 @ 178 mm) stirrups with six vertical legs outside the distance B_C in the cap beam.

$$A_{VO} = \frac{NA_{b\#6}}{S} = \frac{(6)(0.44)}{7/12} = 4.53 \text{ in}^2/\text{ft} \geq A_{VR/ft} \text{ OK}$$

Vertical stirrups inside the pocket connection (A_{Vi}):

$A_{Vi} \geq 0.135A_{st} = 0.135(24)(1.0) = 3.24 \text{ in}^2$ (2090.3 mm^2)

Select 4 #6 (4 #19) stirrups with four vertical legs inside the pocket connection.

$A_{Vi} = (4)(0.44)(4) = 7.04 \text{ in}^2$ (4542 mm^2) $\geq 3.24 \text{ in}^2$ (2090.3 mm^2) OK

The size of the vertical stirrups inside the pocket connection can be potentially reduced; but #6 (#19) bar was selected to be consistent with the design of the vertical stirrups.

- Step 8. Design of diagonal reinforcement

$d_{b\#10} = 1.27$ in (32.26 mm)

$A_{b\#10} = 1.27 \text{ in}^2$ (819 mm^2)

$A_{sb(Cap)} = 12A_{b\#10}$

$A_{s(Diagonal)} \geq A_{sb(Cap)}/6 = 2A_{b\#10} = 2.54 \text{ in}^2$ (1638.7 mm^2)

Select 2 #10 (2 #32) bundled bars at each side of the pocket.

$L_{(Diagonal)} \geq (0.79)(1.27)(68)/\sqrt{5} = 30.5\ in$ (774.7 mm)

Select $L_{(Diagonal)} = 38\ in$ (965.2 mm) according to the detailing in *Fig. 9*.

- Step 9. Principal stress checks

$P_{c(max)} \leq 0.25f'_c = (0.25)(5) = 1.25$ ksi (8.6 MPa)

$P_{t(max)} \leq 0.38\sqrt{f'_c} = 0.38\sqrt{5} = 0.85\ ksi$ (5.9 MPa)

$f_h = 0$, No prestressing force

$$f_v = \frac{P_C}{(B_C + D_{Cap})W_{Cap}} = \frac{800}{(42+60)(72)} = 0.11 \text{ ksi (0.75 MPa)}$$

$$T_C = 0.7A_{st}f_{ye} = (0.7)(24)(1.0)(68) = 1142.4 \text{ kip (5081.6 kN)}$$

$$v_{jv} = \frac{T_C}{(D_P - Gap)(2B_C)} = \frac{1142.4}{(48-2)(2)(42)} = 0.296 \text{ ksi (2.04 MPa)}$$

$$P_c = \left(\frac{f_h + f_v}{2}\right) + \sqrt{\left(\frac{f_h - f_v}{2}\right)^2 + {v_{jv}}^2} = \left(\frac{0+0.11}{2}\right) + \sqrt{\left(\frac{0-0.11}{2}\right)^2 + 0.296^2}$$

$P_c = 0.356$ ksi (2.45 MPa) $\leq P_{c(max)}$ OK

$$P_t = \left|\left(\frac{f_h + f_v}{2}\right) - \sqrt{\left(\frac{f_h - f_v}{2}\right)^2 + {v_{jv}}^2}\right| = \left|\left(\frac{0+0.11}{2}\right) - \sqrt{\left(\frac{0-0.11}{2}\right)^2 + 0.296^2}\right|$$

$P_t = 0.246$ ksi (1.7 MPa) $\leq P_{t(max)}$ OK

$P_t \leq 0.11\sqrt{f'_c} = 0.11\sqrt{5} = 0.246$ ksi (1.7 MPa), no additional bar is necessary in the joint

The depth of the cap beam above the pocket should be checked to avoid punching shear failure above the pocket due to the weight of the cap beam.

A.2 Design example for square column-footing pocket connections

A square bridge column has a clear height of 20 ft (6.1 m) and a cross-sectional dimension of 60x60 in (1524x1524 mm), 40 #10 (40 #32) longitudinal bars, and #5@4 in (#16@101.6 mm) transverse reinforcement with six legs in both directions. The column design axial load, plastic overstrength moment, and shear force corresponding to the plastic overstrength moment are $P_u = 0.06A_g f'_c = 1080$ kips (4804 kN), $M_{PO} = 15900$ k.ft (21557 kN.m), $V_{PO} = 855$ kips (3803 kN). The footing dimension is 18x18 ft (5.48x5.48 m). The maximum moment and shear in the footing are 19000 k.ft (25761 kN.m), and 3390 kips (15079.5 kN), respectively. The nominal and expected compressive strength of concrete are 5 ksi (34.5 MPa) and 6.5 ksi (44.8 MPa). The nominal and expected yield stresses of the steel reinforcement are 60 ksi (414 MPa), and 68 ksi (469 MPa), respectively. The cover concrete in the footing is 3 in (76.2 mm). The final design of the column-footing pocket connection is shown in *Fig. 10*.

- Step 1. Determine the minimum pocket dimension (B_P)

Select $\text{Gap} = 2$ in (51mm), $B_P = 60 + 2(2) = 64$ in (1625.6 mm)

- Step 2. Determine the minimum pocket depth (D_P)

$d_{b\#10} = 1.27$ in (32.26 mm)

$$D_p \geq \begin{cases} 60 + 2 = 62 \text{ in (1574.8 mm)} \\ \dfrac{0.79\,(1.27)(68)}{\sqrt{5}} + 2 = 32.5 \text{ in (825.5 mm)} \\ \dfrac{1.56(855) + \sqrt{4.74\,(855^2) + 6.22(15900 \times 12)(5)(60)}}{(60)(5)} + 2 \\ = 69.6 \text{ in (1767.8 mm)} \end{cases}$$

Select $D_P = 70$ in (1778 mm)

- Step 3. Determine the minimum footing depth ($D_{Footing}$)

$D_{Footing} = 1.25(70) = 87.5$ in (2222.5 mm)

Select $D_{Footing} = 88$ in (2235.2 mm)

- Step 4. Design of footing longitudinal reinforcement

Top bars in the footing should satisfy shrinkage and temperature reinforcement according to AASHTO LRFD Bridge Design Specifications (2010) section 5.10.8.

$$A_{s(Top)} = \frac{1.3B_{Footing}D_{Footing}}{2(B_{Footing} + D_{Footing})f_y} = \frac{(1.3)(18 \times 12)(88)}{2(18 \times 12 + 88)(60)} = 0.7\frac{\text{in}^2}{\text{ft}}\ (1481\frac{\text{mm}^2}{\text{m}})$$

$0.11\frac{\text{in}^2}{\text{ft}} \leq \text{A}_{\text{s(Top)}} \leq 0.6\ \frac{\text{in}^2}{\text{ft}}$

$\text{A}_{\text{s(Top)}} = 0.6\frac{\text{in}^2}{\text{ft}}$, $\text{A}_{\text{b\#7}}$=0.6 in^2, Select #7@10 in (#22@254 mm) for the top bars.

According to the section analysis, the effective yield moment of the footing section was calculated with 22 #11 @ 10 in (22 #36 @ 254 mm) for the bottom bars using the nominal material properties.

$\text{M}_{\text{y (eff)}} = 20067\ \text{k.ft}\ (27207.2\ \text{kN.m})$

$\text{M}_{\text{Demand-Footing}} = 19000\ \text{k.ft}\ (25760.5\ \text{kN.m})$

$\text{M}_{\text{y (eff)}} \geq \text{M}_{\text{Demand-Footing}}$ OK

- Step 5. Design of diagonal reinforcement

$\text{A}_{\text{b\#7}} = 0.6\ \text{in}^2\ (387\ \text{mm}^2)$

$\text{A}_{\text{st(Footing)}} = 16\text{A}_{\text{b\#7}}$

$\text{A}_{\text{s(Diagonal)}} \geq \text{A}_{\text{st(Footing)}}/6 = 2.67\text{A}_{\text{b\#7}} = 1.6\ \text{in}^2\ (1032.2\ \text{mm}^2)$

$\text{d}_{\text{b\#8}} = 1.0\ \text{in}\ (25.4\ \text{mm})$

$\text{A}_{\text{b\#8}} = 0.8\ \text{in}^2\ (516.1\ \text{mm}^2)$

$\text{A}_{\text{s(Diagonal)}} = 2\text{A}_{\text{b\#8}} \geq 1.6\ \text{in}^2\ (1032.2\ \text{mm}^2)$ OK

$\text{Spacing} = 4\text{d}_{\text{b\#8}} = 4.0\ \text{in}\ (101.6\ \text{mm})$

Select 2 #8 @ 4 in (2 #25 @ 101.6 mm) at each corner of the pocket.

$\text{L}_{\text{(Diagonal)}}/2 \geq (0.79)(1.0)(68)/\sqrt{5} = 24\ in\ (609.6\ mm)$

Select $\text{L}_{\text{(Diagonal)}} = 104\ in\ (2641.6\ mm)$, according to the detailing in *Fig. 10*, place the diagonal bars at the top reinforcement and 45 degree around the pocket.

- Step 6. Resistance to overturning

The overturning demand in the footing should satisfy section 6.3.4 of AASHTO [16].

- Step 7. Resistance to sliding

The lateral demand due to the plastic overstrength shear of the column should satisfy section 6.3.5 of AASHTO [16].

- Step 8. Shear design

The footing should satisfy sections 6.3.7 and 6.4.7 of AASHTO for the shear design [16].

- Step 9. Principal stress checks

Footing to column moment resisting joints should satisfy the requirements of section 6.4.5 of AASHTO [16].

The depth of the footing below the pocket should be checked to avoid punching shear failure in the footing due to the weight of the column.

A.3 Design example for unbonded CFRP tendons for post-tensioned bridge columns

Unbonded CFRP tendons are designed for the square bridge column described in the design example A.2. The tensile elastic modulus of CFRP tendons is 21,030 ksi (145 GPa), and the guaranteed tensile capacity is 217 ksi (1496.2 MPa). The cover concrete of the column is 2 in (50.8 mm). The confined properties of the column are as follows:$f'_{cc} = 6.75$ ksi (46.5 MPa), $\varepsilon_{cc} = 0.006$, $f'_{cu} = 4.5$ ksi (31 MPa), $\varepsilon_{cu} = 0.03$. The steel yield strength, f_y, is 60 ksi (413.7 MPa). The steel ultimate strength, f_u, is 90 ksi (620.5 MPa). The steel strain at the beginning of strain hardening, ε_{sh}, is 0.015, and the steel strain at maximum stress, ε_{su}, is 0.12. The final design of the post-tensioned column with CFRP tendons is shown in *Fig. 11*.

- Step 1. Determine the initial post-tensioning stress (f_{pi})

$f_{u(CFRP)} = 217$ ksi (1496.2 MPa)

$f_{pi} = 0.25 f_{u(CFRP)} = (0.25)(217) = 54.25$ ksi (374 MPa)

- Step 2. Determine the area of CFRP Tendons (A_{CFRP})

$$A_{CFRP(total)} = ALIf'_c A_g / (0.25 f_{u(CFRP} = (0.06)(5)(60 \times 60)/(54.25) = 19.91 \text{ in}^2 \ (12845.1 \text{ mm}^2)$$

$A_{CFRP} = 1.24\ in^2\ (800\ mm^2)$

$n = A_{CFRP(total)}/A_{CFRP} = 16$

Select 16 CFRP 1x37 tendons

- Step 3. Pushover analysis

After performing pushover analysis, the column model reaches a drift ratio of 6.5% at column failure. The maximum tensile stress in the CFRP tendons at the column failure was as follow:

$f_{max(CFRP)} = 156$ ksi(1075.6 MPa) $\leq 0.8 f_{u(CFRP)} = 173.6$ ksi(1197 MPa)

$$\frac{f_{max(CFRP)}}{f_{u(CFRP)}} = 72\% < 80\%\ OK$$

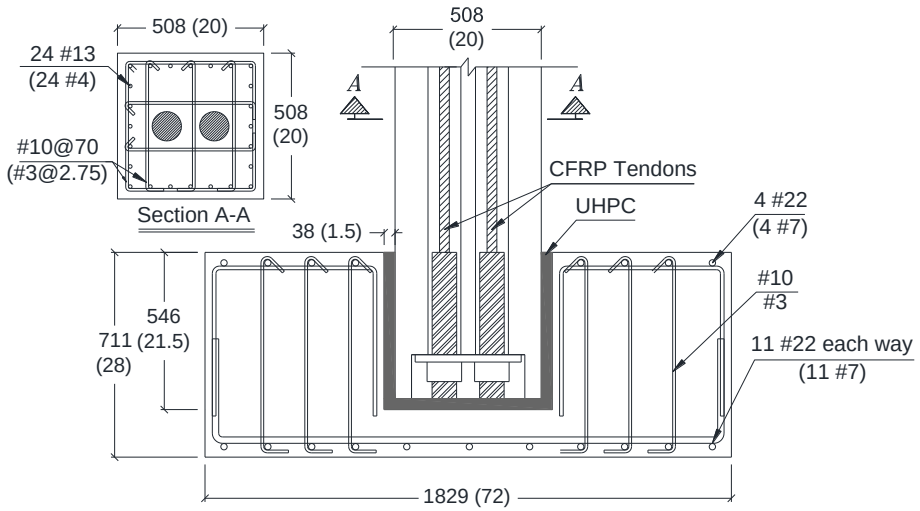

Figure 1. Details of the column-footing pocket connection of the single column model [units are mm (in)]

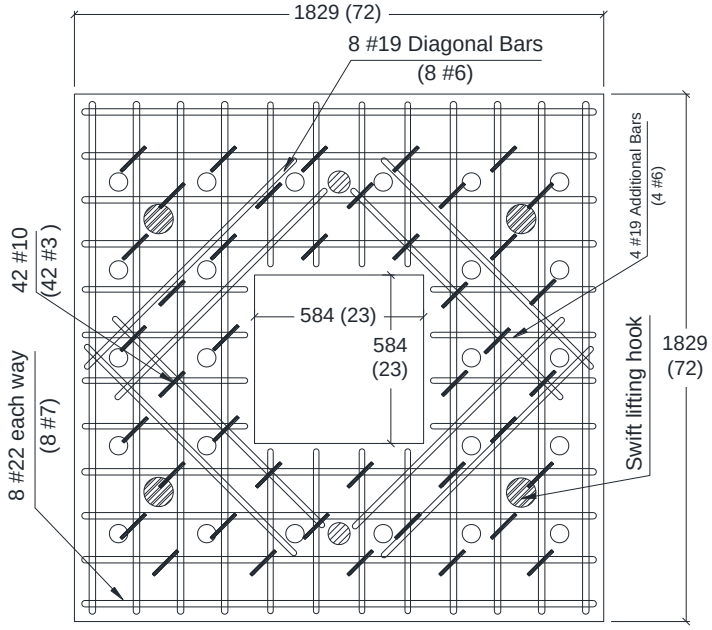

Figure 2. Details of the top reinforcement in the footing of the single column model [units are mm (in)]

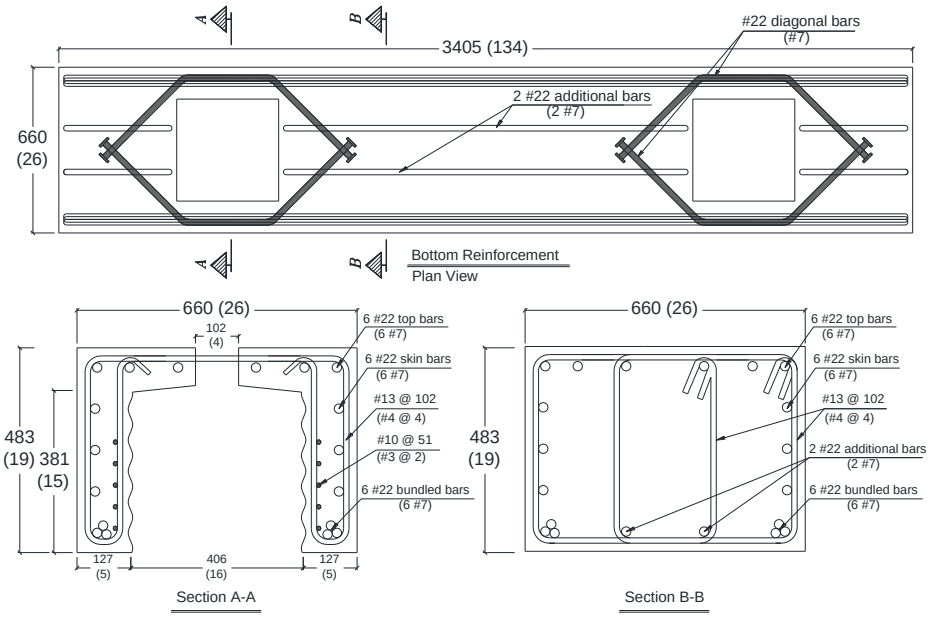

Figure 3. Details of the cap beam reinforcement of the two-column bent model [units are mm (in)]

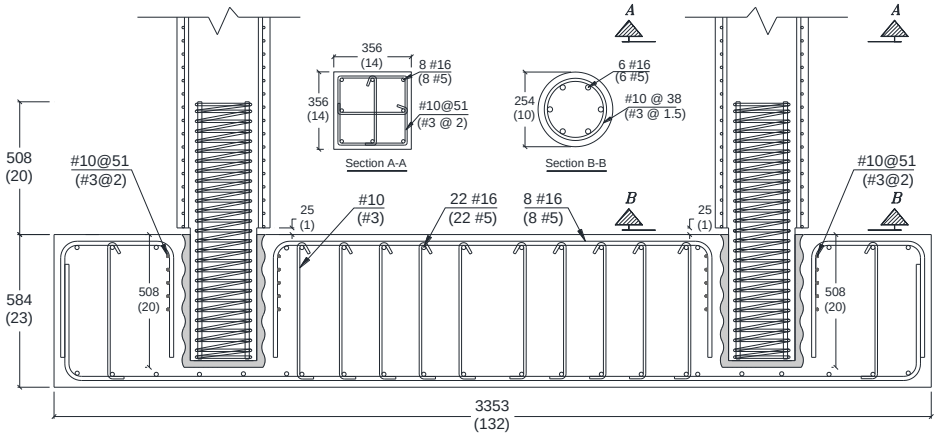

Figure 4. Details of the footing reinforcement of the two-column bent model [units are mm (in)]

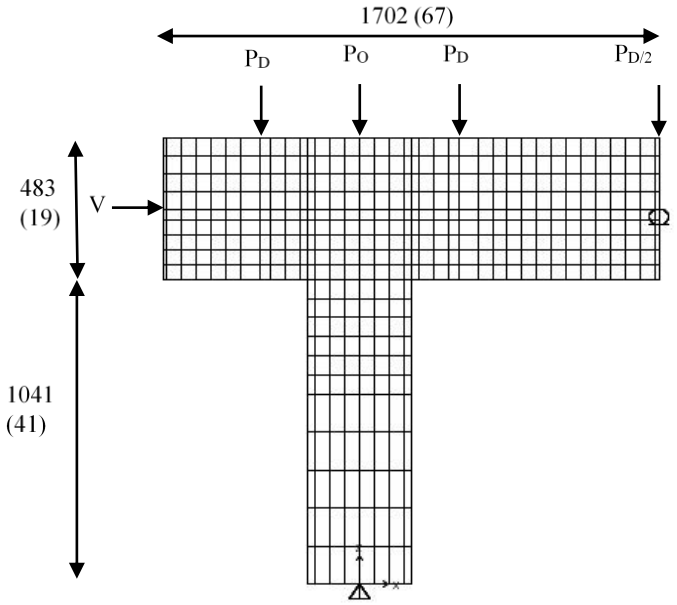

Figure 5. Analytical model details of the column-cap beam connection [units are mm (in)]

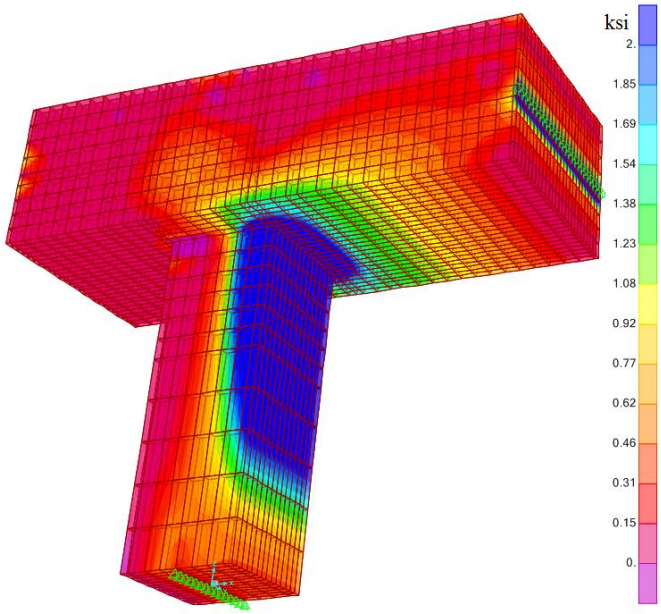

(a)

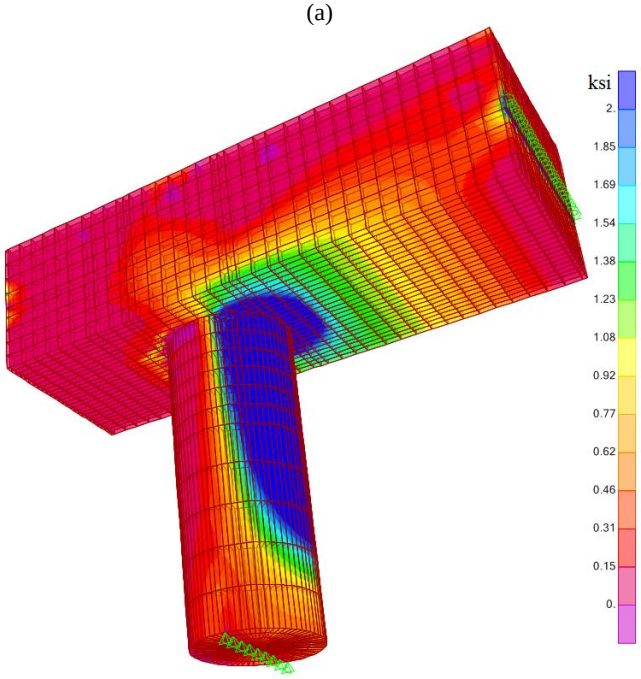

(b)

Figure 6. Contour of the maximum tensile stress (a) square (b) circular columns [1 ksi = 6.9 MPa]

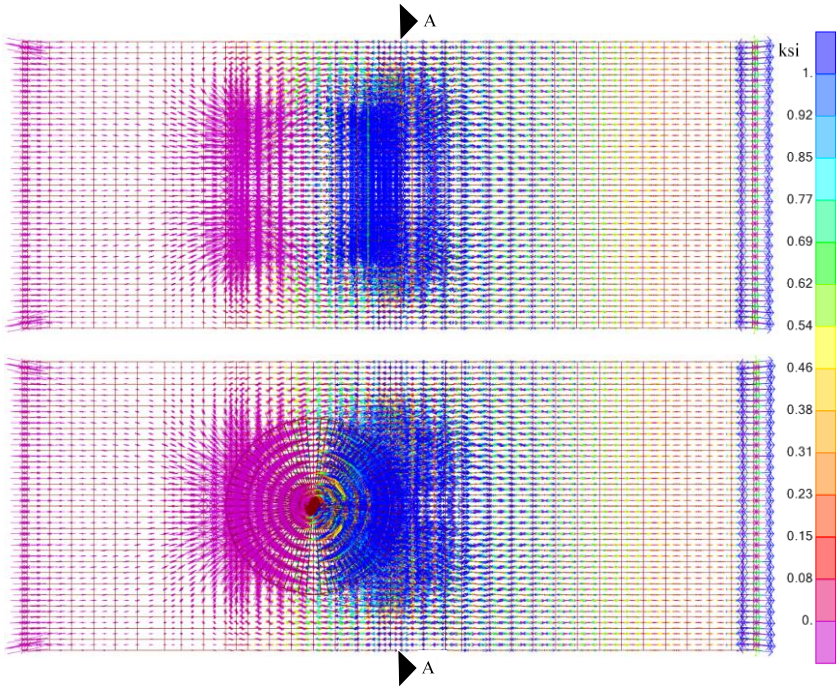

Figure 7. Maximum tensile stress at the column-cap beam interface [1 ksi = 6.9 MPa]

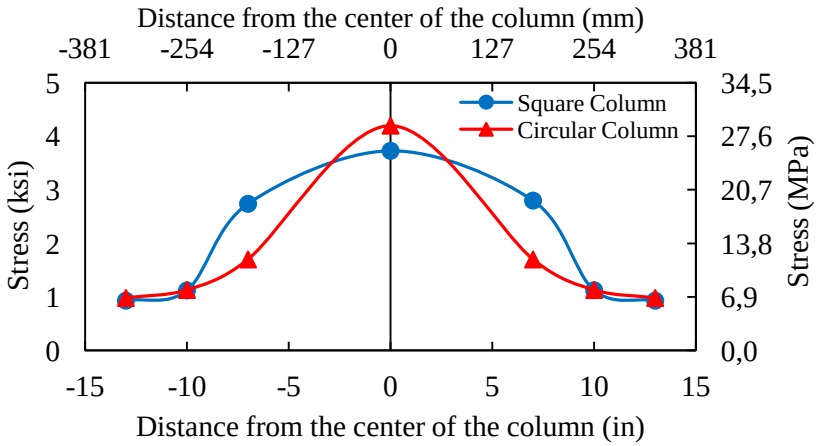

Figure 8. Maximum tensile stress in section A-A at the interface for square and circular columns

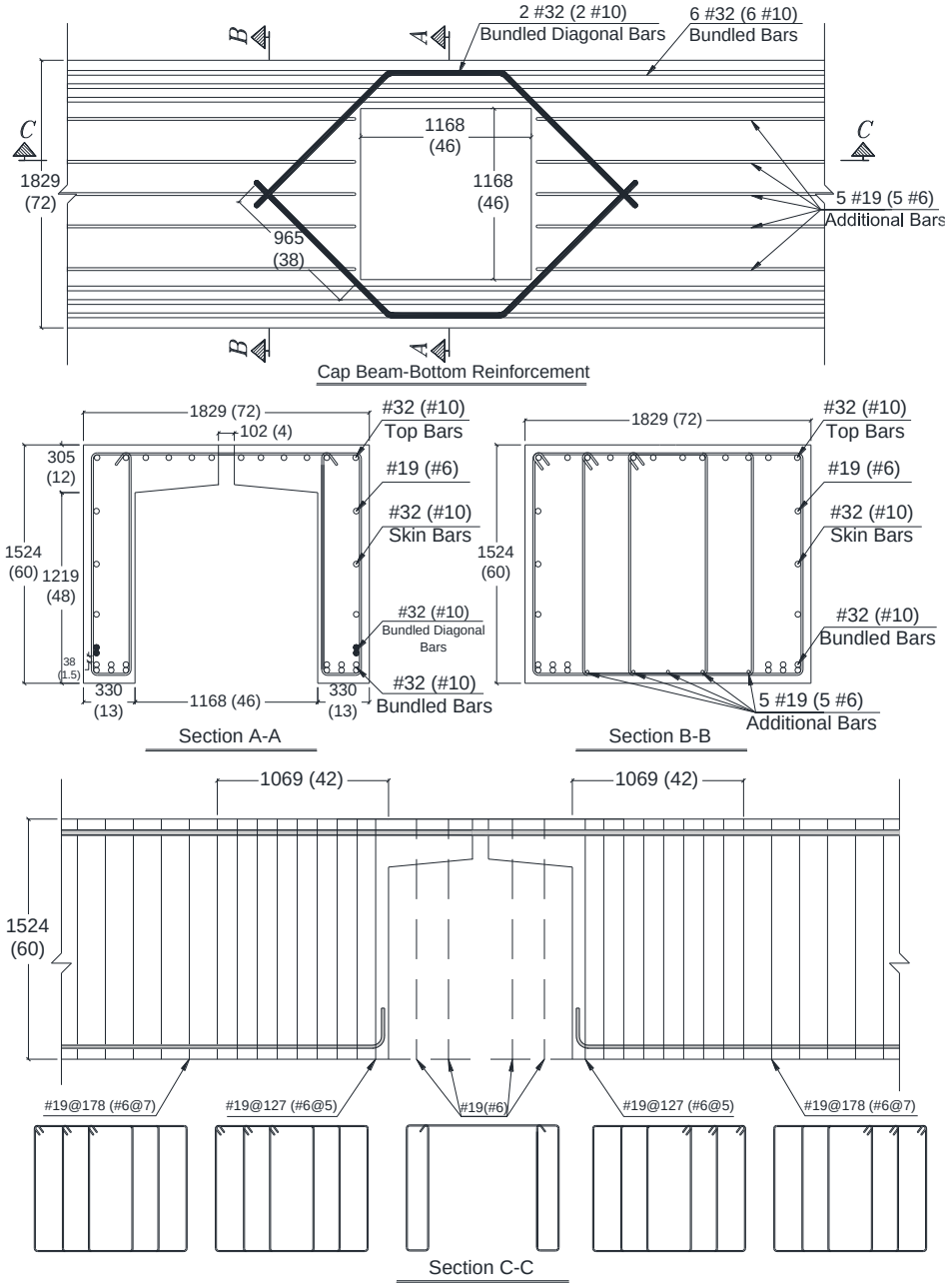

Figure 9. Details of square column-cap beam pocket connection [units are mm (in)]

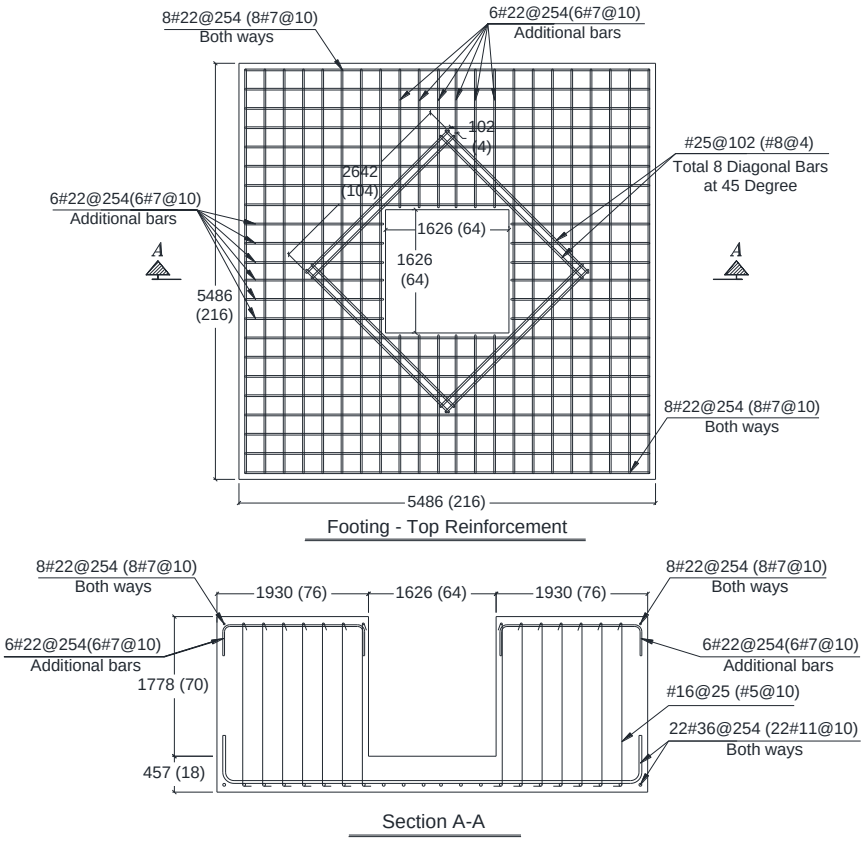

Figure 10. Details of square column-footing pocket connection [units are mm (in)]

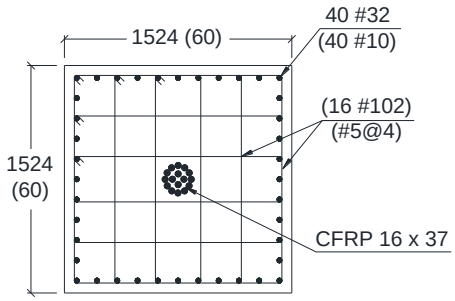

Figure 11. Cross-section of the post-tensioned column using CFRP tendons [units are mm (in)]